We are IntechOpen, the world's leading publisher of Open Access books Built by scientists, for scientists

4,800
Open access books available

122,000
International authors and editors

135M
Downloads

Our authors are among the

154
Countries delivered to

TOP 1%
most cited scientists

12.2%
Contributors from top 500 universities

WEB OF SCIENCE™

Selection of our books indexed in the Book Citation Index in Web of Science™ Core Collection (BKCI)

Interested in publishing with us?
Contact book.department@intechopen.com

Numbers displayed above are based on latest data collected.
For more information visit www.intechopen.com

6

Kinematics Synthesis of a New Generation of Rapid Linear Actuators for High Velocity Robotics with Improved Performance Based on Parallel Architecture

Luc Rolland
Ecole Normale Supérieure des Arts et Métiers, Metz
France

1. Introduction

This article studies several classes of linear actuators based on parallel topology featuring lower mobility.
Translation actuator design represents a very important issue in manipulator design in areas like machine tools for example and more recently hexapods. Actual designs are usually limited to low accelerations actually limited to 2 g. Moreover, alignment problems are difficult to circumvent and usually lead to non-uniform friction in the translation motion refered as hard spots. Despite important breakthroughs, linear motors are still limited to accelerations of 5g and they are plagued by problems such as surrounding magnetisation and limited torque. As for any parallel mechanisms, the proposed architectures do provide for a more rigid linkage. Their rigidity advantage leads to larger actuator bandwidth, thereby allowing for increased accelerations which result in larger forces being applicable to the extremity while keeping overall mass very low. The main disadvantage will be their transverse emcumbrance which will be minimized through mechanism networking.
Two diamond and one rhombus configurations have been designed, analyzed, constructed and compared verifying their ability for very fast accelerations. Their kinematics are investigated allowing to write the forward and inverse problems for position, velocity and accelerations where closed-form solutions are determined. Motion limitations and singularity analysis are also provided from which configuration recommendations can be derived. These actuators will then be easily controllable despite their non-linear nature.
In parallel manipulators, the prismatic pairs are usually encountered as the linear actuators for several architectures such as the planar 3RPR, the general Gough platform, (Gough & Whitehall, 1962; Fichter, Kerr and Rees-Jones) and the Kanuk (Rolland, 1999) for examples.
These prismatic actuators, may they be guided or not, do play a very important role in robotics design and their performance has been an issue. According to the author's obsevration on several high speed milling projects, these actuators have been hampering the advent of high speed milling by being unable to provide for adequate accelerations in low inertia and high rigidity packages.

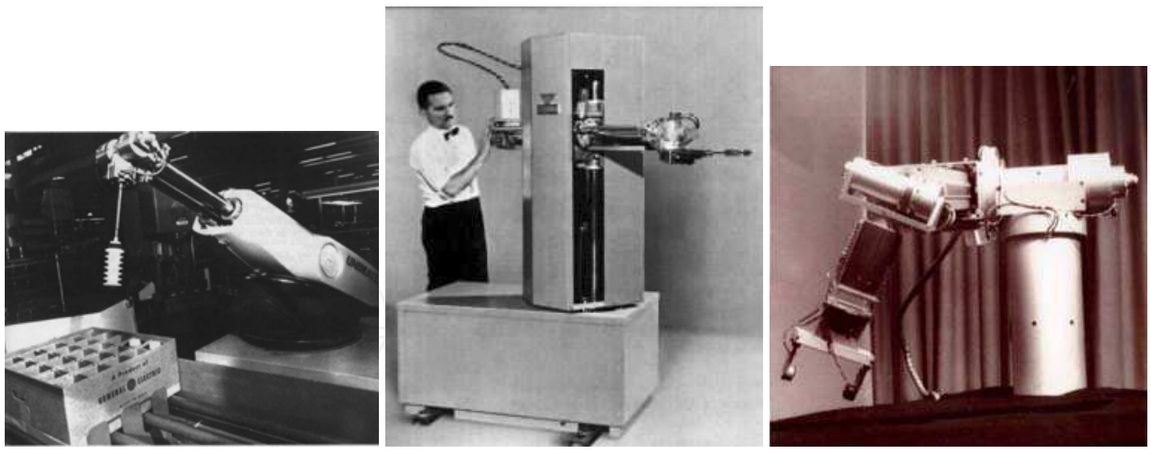

(a) Unimate (b) Versatran (c) Stanford Arm

Fig. 1. Cylindrical robots

Typically, contemporary linear actuators have generally evolved in devices which can be classified under the nine following categories:

- Piston in a Cylinder or diaphragm being driven by a fluid
- Linear motors
- machine screw and nut
- A worm gear and screw
- Rack and pinion
- Belts and pulleys
- Cam and plunger
- Crank-slider
- Linkages

Lets consider Euclid's definition of a straight line: "A straight line is a line which lies evenly with the points on itself", (Euclid, 2002).

A straight line mechanism is defined as a mechanism that generates a straight-line output motion from an input actuator which rotates, oscillates, or moves in a straight line.

Inventing a straight line mechanism, referred as SLM hereafter, has been the concern of many researchers and engineers long before the industrial revolution. The use of linkages as SLM can be traced as far back as in the XIII century when sawmill drawings showed mechanisms for changing circular motion to straight-line motion. Even Da Vinci himself has drawn one mechanism to convert rotation to translation having slides acting as guides (DaVinci, 1493). Door locking mechanisms are other old examples where the rotation of the key was converted into translation motion of the lock element.

In 1603, Christopher Scheiner invented the pantograph, (Scheiner, 1631). It may be regarded as the first example of the four-bar linkage. The pantograph is a device for copying and enlarging drawings. Knowing that the actuator is located to one end, this device can be made to move on a straight-line providing that the input follows a straight-line, therefore becoming a pure amplification linkage.

In the late seventeenth century, it was extremely difficult to machine straight line and flat surfaces. Knowing that prismatic pair construction without backlash had become an important and difficult challenge, much effort was then diverted towards the coupler curve of a linkage comprising only revolute joints which were much easier to produce.

Fig. 2. Typical linear actuator

Later, James Watt proposed a four-bar mechanism generating motion approximating roughly a straight-line. We would have to wait until 1864 when Peaucellier introduced the first planar linkage capable of transforming rotary motion into exact straight-line motion. Until this invention, no planar mechanism existed for producing straight-line motion without reference guideways which could not be made very straight themselves.
It was soon followed by the grasshopper linkage which also provided for an exact straight-line. These mechanisms were essential in the development of steam engines and machine tools. Then, Hart's Linkage and A-frame both reduce the link number to only five.
The Kmoddl library from Cornell University presents 39 linkages imagined to produce linear motion which come from Franz Reuleaux Collection of Kinematic Mechanisms (Reuleaux, 1876; Moon, 2007). Most of them feature relatively complex architectures where linkages cannot easily be practically applied in systems such as robots or milling machines.
Several proposals were patented trying to simplify the linkage producing straight-line motion. In the class of nearly straight line linkages, one can identify several linkages by inventors such as Hoekens, Chebyshev, Evans, Roberts and Burmester. With appropriate linkage dimensions, part of the motion can be a straigth line. Hoekens linkage can be considered a Cognate linkage of the Chebyshev linkage since it produces a similar motion pattern. These simpler designs always applied the properties of special points on one of the links of a four-bar linkage. They could often produce straight-lines over some limited range of their motion. The commonality of all these ingenious mechanisms is in the fact that they feature linkages based on closed loops or so-called parallel topology.
Very early on, the designers were faced with the fact that a prismatic pair or joint is much more difficult to build than a revolute joint. This is even more the case when trying to have a linear actuator, (Soylemez, 1999). This observation holds on even today.
Practically, parallel mechanism architectures have been able to provide solutions to industrial problems and needs with improved performance manipulators.
Theoritically, they may even improve accuracy but this is still an open problem at the moment, especially when control in concerned.
When the proposed configurations allow to bring the actuators fixed on or jointed to the base, the inertia of mobile elements can be significantly reduced so the extremity or end-effector can move at higher accelerations resulting in the deliverance of larger forces.

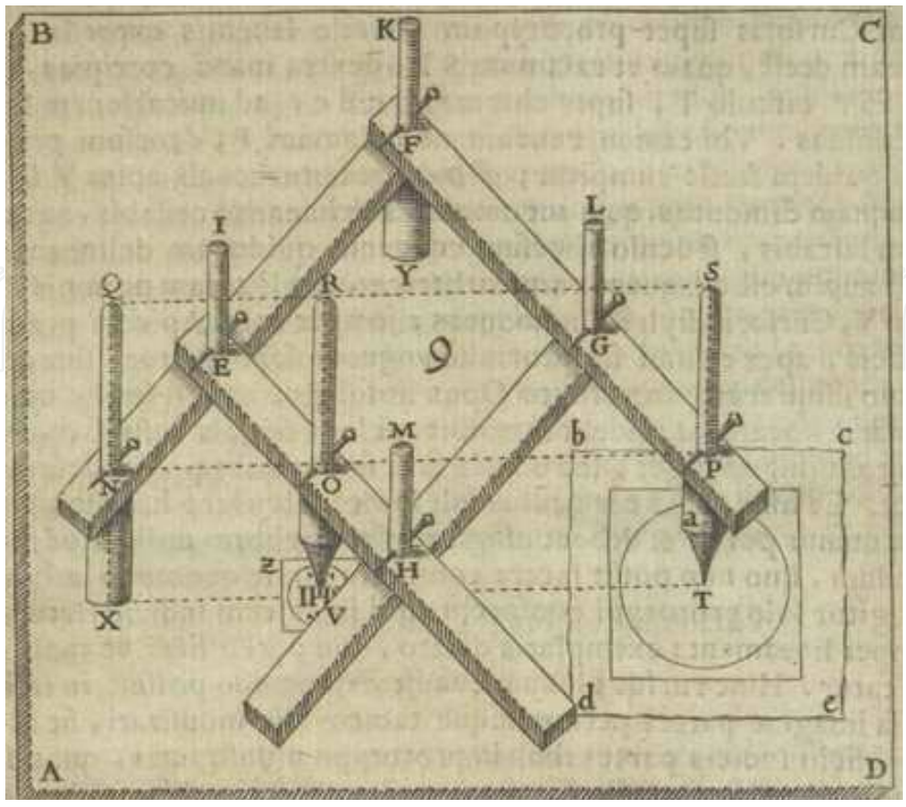

Fig. 3. Scheiner pantograph

The principal drawback which shall be studied is the construction of kinematics models characterized by non-linear equations where an implicit relationship is produced between the manipulator configuration parameters, actuator joint positions and the end-effector position and orientation.

The simplest forms of parallel manipulators are the ones producing one degree-of-freedom. Performance evaluation for these single DOF mechanisms includes the four following criterias:

- workspace
- singularity avoidance
- linkage ecumbrance
- linearity in motion transmission

In a one DOF problem, the workspace criteria is then reduced to a simple range with two extremum values te be determined: the minimal and maximal positions.

Moreover, the design of machine-tools based on parallel robots have been concerned by problems related to inherent difficulties with prismatic actuator designs which have hampered their successful implementation.

This paper original contribution is in the design of a new generation of linear actuators for increased performance where planar parallel linkages are applied. For example, if implemented to replace classical linear actuators on Gough platform or even planar 3RPR manipulators, they allow to bring the motors in positions directly jointed to the base.

The introduction is followed by chapter on kinematic topology synthesis consisting of a review of various kinds of mechanisms to provide straight-line motion where mobility is

analyzed. Chapter 3 is dedicated to the kinematics analysis of several promising alternatives based on the four-bar mechanism. Then, chapter four investigates the selected performance criterias. This paper closes on a design chapter where prototypes are shown with motion analysis in terms of position, velocity and acceleration.

2. Kinematics topology synthesis

Firstly, in this section, we shall make a review of some interesting planar mechanisms which can perform the specified set of functionnal requirements. In this case the tasks shall be to achieve straight-line motion.

2.1 Background study

We need two definitions related to degree-of-freedoms.
The DOF of the space is defined as the number of independant parameters to define the position of a rigid body in that space, identified as λ.
The DOF of a kinematic pair is defined as the number of independant parameters that is required to determine the relative position of one rigid body with respect to the other connected rigid body through the kinematic pair.
The term mechanism is defined as a group of rigid bodies or links connected together to transmit force and motion.
Mobility and kinematics analyses are possible under some assumptions:

- Ideal mechanisms with rigid bodies reducing the mechanism motion to the geometric domain.
- Elastic deformations are neglected
- Joint clearance and backlash are insignificant

2.2 Functionnal requirements

Historically, the need for straight-line motion has resulted on linkages based on closed loops or so-called parallel topology. The idea is to convert rotation motion into translations or straight-line motions. It is usually considered that prismatic pairs are much harder to build than revolute joints, (Soylemez, 1999).
Prismatic actuators as well as slides have the following problems:

- the side reactions of prismatic pairs produce friction leading to wear
- these wears are uneven, non-uniform and unpredictable along the path of the slide since the flat surfaces in contact are not well defined due to construction imperfections.

Some mechanisms are designed to generate a straight-line output motion from an input element which rotates, oscillates or moves also in a straight line.
The kinematic pair DOF is defined as the number of independent parameters necessary to determine the relative position of one rigid body with respect to the other connected to the pair, (Soylemez, 1999).
The linkages are designed to generate motion in the plane and are then limited to three DOFs, therefore the only available joints are either with one or 2 dofs only.
The actual problem is addressed from a robotics or even machine-tool point of view. It can be summarized by this question: how can you draw a straight line without a reference edge? Most robotics manipulators or machine tools are applying referenced linear motions with guiding rails and even now linear motors. In design of parallel manipulators such as 3RPR

or Gough platforms, the actuators have especially to generate straight lines without any guiding rails.
This question is not new and it actually comes from the title taken from the book written by Kempe, where he describes plane linkages which were designed to constrain mechanical linkages to move in a straight line (Kempe, 1877).

2.3 Mobility analysis of linkages

Here is the mobility formula that is applied for topology investigation, (Rolland, 1998):

$$m = \Sigma j_i - \lambda n \tag{1}$$

where Σj_i is the sum of all degree-of-freedoms introduced by joints and $\lambda = 3$ is the available DOF of the planar space in which the actuator is evolving.
Finally, the number of closed loops in the system is n. This number can be multiplied and shall be a natural number $n \in \{1,2,3, \ldots\}$

2.4 Four-bar mechanisms

If $n = 1$ and only revolute joints are selected, then the mechanisms can be selected in the large variety of four-bar mechanisms. These linkages feature one closed-loop or one mechanical circuit. According to Grashof's law, the sum of the shortest and longest link cannot exceed the sum of the remaining two links if there is to be continuous relative motion between the links. Hence, they can be classified as four types as shown in figure 4.

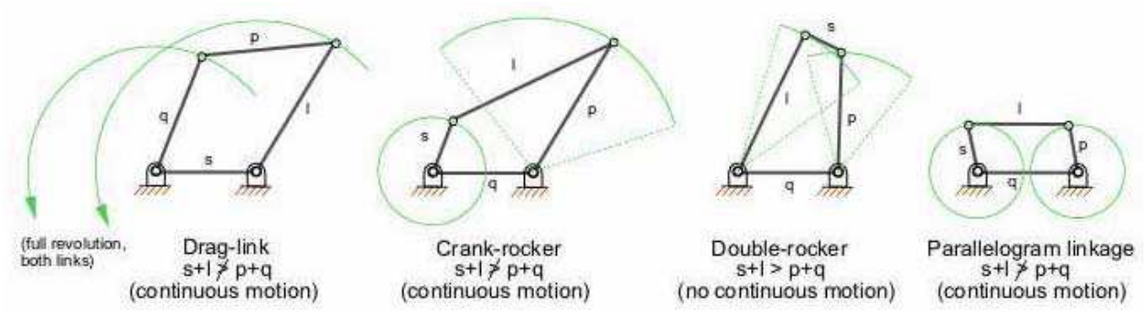

Fig. 4. Four-bar mechanism classification (from Wikipedia)

Three four-bar mechanisms can produce partial straight-line motion. They are characterized by two joints connected to the fixed base.
The Chebyshev linkage is the epitome of the four-bar mechanical linkage that converts rotational motion to approximate straight-line motion. It was invented by the 19th century mathematician Pafnuty Chebyshev. It is a four-bar linkage therefore it includes 4 revolute joints such that $\Sigma j_i = 4 * 1$ where $n = 1$ since there is only one closed loop. The resulting mobility: $m = 4-3 * 1=1$. Hoekens linkage happens to be a Cognate linkage of the Chebyshev linkage. It produces a similar motion pattern. With appropriate linkage dimensions, part of the motion can be an exact straigth line.
Robert's linkage can have the extremity P set at any distance providing it is layed out on that line perpendicular to the coupler, i-e link between A and B. This means that P can be positionned on top of the coupler curve instead of below.

This mobility calculation holds fo any four-bar mechanism including the free ones, i-e not being attached to the base.
If properly designed and dimensionned, four-bar linkages can become straight-line motion generators as will be seen in the next section on kinematics. This is one of the contribution of this work.

2.5 True straight-line mechanisms

If $n > 1$ and only revolute joints are selected, then the mechanisms become more complex and will integrate two closed loops or two mechanical circuits.
Three mechanisms can produce exact straight-line motion: the Peaucelier linkage, the Grasshoper mechanism and a third one which has no name.
This linkage contains nine revolute joints such that $\Sigma j_i = 9 * 1 = 9$. Please note that where three links meet at one point, two revolute joints are effectively existing. Three closed loops can be counted for $n = 3$. The resulting mobility: $m = 9 - 3 * 3 = 0$. The linkage designed by Peaucelier is one of those mechanisms which cannot meet the mobility criterion but do provide the required mobility. Very recently, Gogu has reviewed the limitations of mobility analysis, (Gogu, 2004).

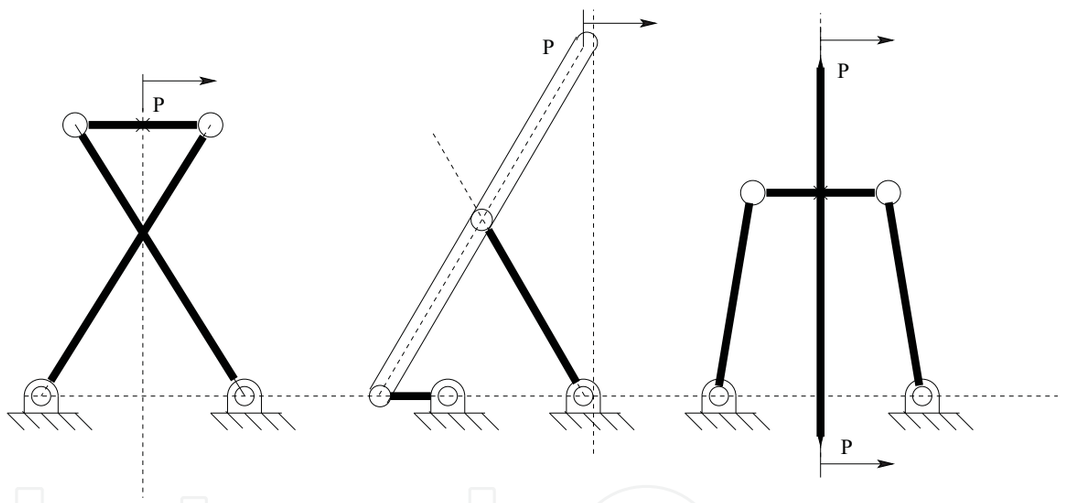

Fig. 5. Four-bar mechanisms: Chebyshev, Hoekens and Robert linkages

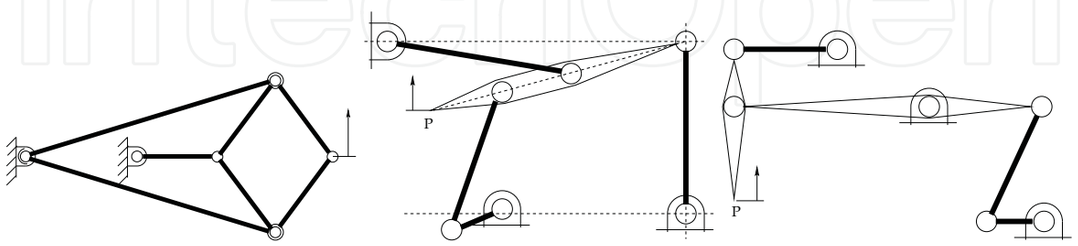

(a) Peaucelier (b) The grasshoper (c) An alternate case

Fig. 6. Exact straigth-line mechanisms

The two other linkages do provide for seven revolute joints for $\Sigma j_i = 7 * 1 = 7$ and two closed loops for $n = 2$. The resulting mobility: $m = 7 - 3 * 2 = 1$ which is verified by experiments.

These three mechanisms do provide for straight-line motion at the cost of complex linkages which do occupy very valuable space. This makes them less likely to be applied on robots.

3. Kinematics analysis

A mechanism is defined as a group of rigid bodies connected to each other by rigid kinematics pairs to transmit force and motion. (Soylemez, 1999).
Kinematics synthesis is defined as the design of a mechanism to yield a predetermined set of motion with specific characteristics.
We shall favor dimensional synthesis of function generation implementing an analytical method. The function is simply a linear function describing a straight-line positioned parallel to one reference frame axis.
The method will implement a loop-closure equation particularily expressed for the general four bar linkage at first. The first step consists in establishing the fixed base coordinate system.

3.1 Four-bar mechanism

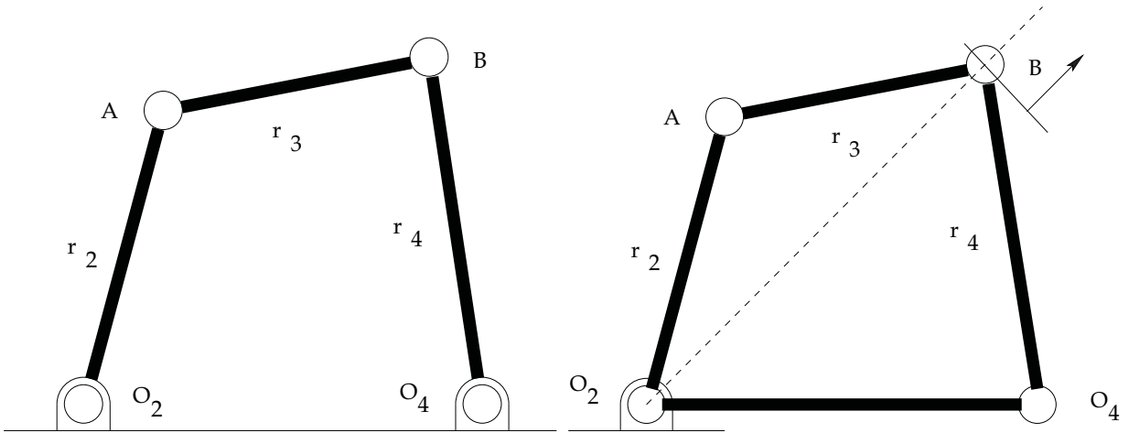

(a) Fixed four-bar (b) Semi-free four-bar

Fig. 7. General four-bar linkages

Lets define the position vectors and write the vector equation. Taking O_2 and O_4 as the link connecting points to the fixed base located at the revolute joint center, taking A and B as the remainder mobile revolute joint centers, the general vectorial formulation is the following, (Uicker, Pennock and Shigley, 2003):

$$(r_1 + r_2 + r_3 + r_4 = 0) \tag{2}$$

This last equation is rewritten using the complex algebra formulation which is available in the textbooks, (Uicker, Pennock and Shigley):

$$r_1 e^{j\theta_1} + r_2 e^{j\theta_2} + r_3 e^{j\theta_3} - r_4 e^{j\theta_4} = 0 \tag{3}$$

where θ_1, θ_2, θ_3 and θ_4 are respectively the fixed base, crank, coupler and follower angles respective to the horizontal X axis.
If we set the x axis to be colinear with O_2O_4, if we wish to isolate point B under study, then the equation system becomes:

$$r_3 e^{j\theta_3} = r_4 e^{j\theta_4} - r_1 - r_2 e^{j\theta_2} \tag{4}$$

Complex algebra contains two parts directly related to 2D geometry. We project to the x and y coordinate axes, in order to obtain the two algebraic equations. The real part corresponds to the X coordinates and the imaginary part to the Y coordinates. Thus, the equation system can be converted into two distinct equations in trigonometric format.
For the real or horizontal part:

$$r_3 \cos(\theta_3) = r_4 \cos(\theta_4) - r_1 - r_2 \cos(\theta_2) \tag{5}$$

For the imaginary or vertical part:

$$r_3 \sin(\theta_3) = r_4 \sin(\theta_4) - r_2 \sin(\theta_2) \tag{6}$$

When O_2O_4 is made colinear with the X axis, as far as r_1 is concerned, there remains only one real part leading to some useful simplification.
The general four bar linkage can be configured in floating format where the O_4 joint is detached from the fixed base, leaving one joint attached through a pivot connected to the base. Then, a relative moving reference frame can be attached on O_2 and pointing towards O_4. This change results in the same kinematic equations.
Since, the same equation holds and we can solve the system:

$$(\theta_4) = 2\arctan\left(\frac{B + -\sqrt{A^2 + B^2 - C^2}}{A + C}\right) \tag{7}$$

where the A,B,C parameters are:

$$\begin{aligned} A &= \frac{r_1}{r_2} - \cos(\theta_2) \\ B &= -\sin(\theta_2) \\ C &= \frac{r_1 \cos(\theta_2)}{r_4} - \frac{1}{2}\frac{r_1^2 + r_2^2 - r_3^2 + r_4^2}{r_2 r_4} \end{aligned} \tag{8}$$

To determine the position of joint center B in terms of the relative reference frame O:

$$O_2B = [r_1 + r_4 \cos(\theta_4), r_4 \sin(\theta_4)]^t \tag{9}$$

Then, the norm of the vector OB gives the distance between O and B:

$$x = |O_2B| = \sqrt{\left(r_1 + r_4 \cos(\theta_4)\right)^2 + r_4^2 \left(\sin(\theta_4)\right)^2} \tag{10}$$

This explicit equation gives the solution to the forward kinematics problem. An expression spanning several lines if expanded and which cannot be shown here when the expression of θ_4, equation 7, is substitued in it. This last equation gives the distance between O and B, the output of the system in relation to the angle θ_2, the input of the system as produced by the rotary motor. The problem can be defined as: **Given the angle θ_2, calculate the distance x between O and B.**

The four-bar can be referred as one of the simplest parallel manipulator forms, featuring one DOF in the planar space ($\lambda = 3$). One family of the lowest mobility parallel mechanisms.
The important issue is the one of the path obtained by point B which is described by a coupler curve not being a straight line in the four-bar general case.
However, in the floating case, if applied as an actuator, the general four-bar can be made to react like a linear actuator. The drawbacks are in its complex algebraic formulation and non-regular shape making it prone for collisions.

3.2 Specific four bar linkages

We have two questions if we want to apply them as linear actuators:

- Can we have the four-bar linkage to be made to move in a straight-line between point O_2, the input, where the motor is located and B, the output, where the extremity or end-effector is positionned?
- Can simplification of resulting equations lead to their inversions?

As we have seen earlier, specific four bar linkages can be made to produce straight-line paths if they use appropriate dimensions and their coupler curves are considered on link extensions. In this case, we still wish to study the motion of B with the link lengths made equal in specific formats to produce specific shapes with interesting properties. Three solutions can be derived:

- the parallelogram configuration,
- the rhombus configuration,
- the kite or diamond shape configuration, (Kempe, 1877).

3.2.1 The parallelogram configuration

Parallelograms are characterized by their opposite sides of equal lengths and they can have any angle. They even include the rectangle when angles are set to 90 degrees. They have been applied for motion transmission in the CaPaMan robot, (Ceccarelli, 1997).
The parallelogram four-bars are characterized by one long and one short link length. They can be configured into two different formats as shown in figure 8.

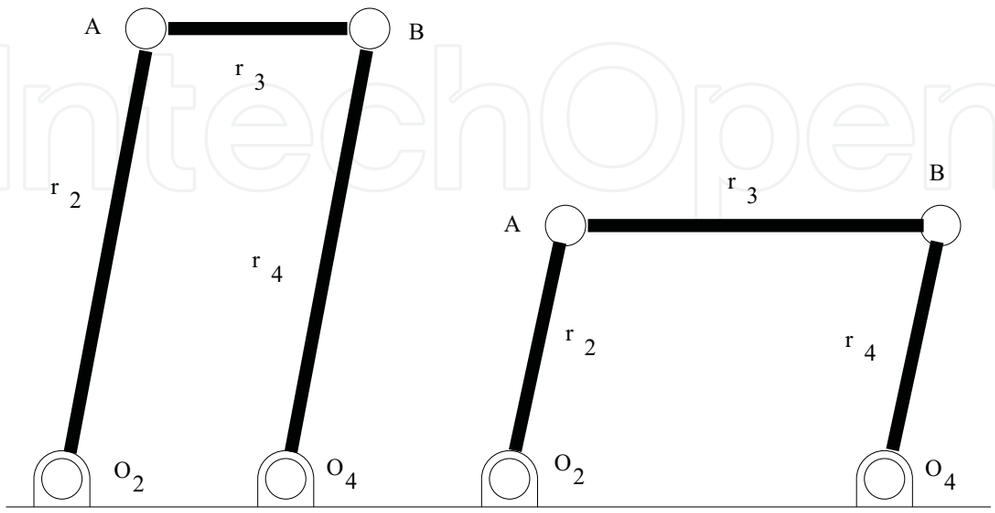

Fig. 8. The two parallelogram four-bar cases

The follower follows exactly the crank. This results in the equivalence of the input and following angles: $\theta_4 = \theta_2$.
If we set R and r as the link lengths respectively, then to determine the position of joint center B in terms of the relative reference frame O_2; an simple expression is derived from the general four-bar one:

$$O_2B = [R + r\cos(\theta), r\sin(\theta)] \tag{11}$$

Then, the norm of the vector O_2B gives the distance between O_2 and B:

$$x = |O_2B| = \sqrt{R^2 + r^2 + 2Rr\cos(\theta)} \tag{12}$$

This last equation is the result of the forward kinematics problem.
Isolation of the θ variable will lead to the inverse kinematics problem formulation:

$$\theta = \arccos\left(\frac{x^2 - R^2 - r^2}{2Rr}\right) \tag{13}$$

Detaching joint O_4 from the fixed base, the parallelogram becomes a semi-free linkage which can be considered as one prismatic actuator.

3.2.2 The rhombus configuration

The rhombus configuration can be considered a special case of the parallelogram one. All sides of a Rhombus are congruent and they can have any angle. Therefore, $r_1 = r_2 = r_3 = r_4$ or even one can write $r = R$ as for the parallelogram parameters. The mechanism configuration even includes the square when angles are set to 90 degrees.
The forward kinematics problem becomes:

$$x = 2r\cos\left(\frac{\theta}{2}\right) \tag{14}$$

The Inverse kinematics problem is expressed as:

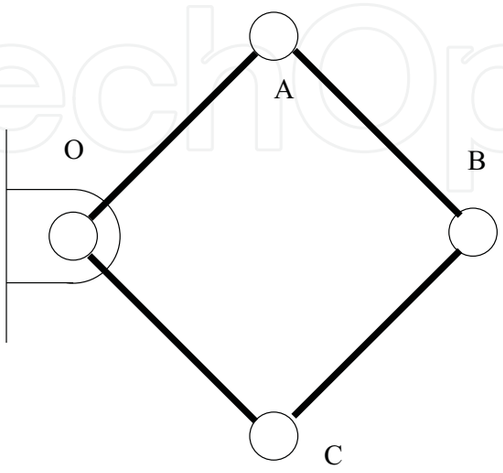

Fig. 9. The Rhombus detailed configuration

$$\theta = 2\arccos\left(\frac{x}{2r}\right) \tag{15}$$

Simple derivation will lead to differential kinematics.
The forward differential kinematics is expressed by the following equation:

$$v = -r\omega\sin(\frac{\theta}{2}) \tag{16}$$

where $\omega = \frac{d\theta}{dt}$

We take the following geometric property:

$$\cos\left(\frac{\theta}{2}\right) = \frac{x}{2} \tag{17}$$

We apply Pythagore's theorem:

$$\sin\left(\frac{\theta}{2}\right) = \frac{1}{2}\sqrt{4 - \frac{x^2}{r^2}} \tag{18}$$

Then, the FDP can be rewritten in terms of the length x:

$$v = -\omega\frac{r}{2}\sqrt{4 - \frac{x^2}{r^2}} \tag{19}$$

Inversion of equation 19 lead to the inverse differential kinematics problem being expressed as:

$$\omega = -\frac{v}{r\sin(\frac{\theta}{2})} \tag{20}$$

Substituting equation 17 and equation 18 into the former, we obtain:

$$\omega = -\frac{v}{r}\sqrt{1 - \frac{x}{2r}} \tag{21}$$

Further derivation will give the extremity acceleration where the FDDP can be expressed as:

$$a = -r\alpha\sin\left(\frac{\theta}{2}\right) - \frac{1}{2}r\omega^2\cos\left(\frac{\theta}{2}\right) \tag{22}$$

Substituting equation 17 into the former lead to the following expression of the FDDP:

$$a = -\frac{1}{2}r\alpha\sqrt{4 - \frac{x^2}{r^2}} - \frac{1}{4}\omega^2 x \tag{23}$$

The IDDP:

$$\alpha = \frac{-a - \frac{1}{2} r \omega^2 \cos\left(\frac{\theta}{2}\right)}{r \sin\left(\frac{\theta}{2}\right)} \tag{24}$$

Substituting equation 21, equation 17 and equation 18 into the former, we obtain:

$$\alpha = -2ar^{-1} \frac{1}{\sqrt{4 - \frac{x^2}{r^2}}} - \frac{1}{2} v x \sqrt{2} r^{-4} \left(\frac{x}{r}\right)^{-3/2} \tag{25}$$

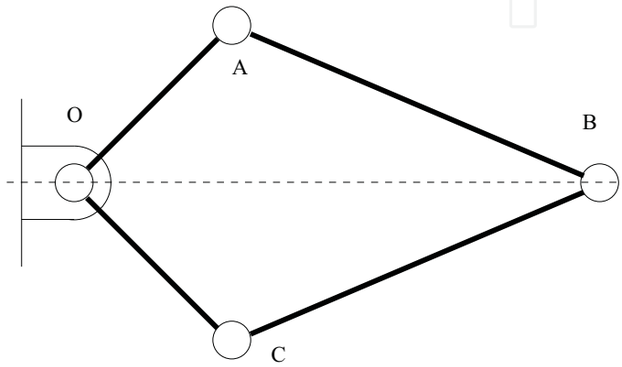

Fig. 10. The diamond shape four-bar

3.2.3 The kite or diamond shape configuration

The kite configuration is characterized by two pairs of adjacent sides of equal lengths, namely R and r.

Then, two configurations into space depending on which joint the motor is attached. The motor is also located on the joint attached on the fixed base.

To obtain the first configuration, the first pair is located at O_2, the crank joint center where the motor is located, as its articulation center and the second pair at B, the extremity joint, as its center.

The second configuration integrates the actuator on O_4. However, the actuator x output is defined as the linear distance between O_2 and B making this actuator moving sideways. The problem will be that the change of four-bar width is going to introduce parasitic transverse motion which will in turn prevent real linear motion due to the pivot effect caused by the motor joint. This approach is thus rejected.

To obtain the second disposition, one can mount the driven joint between two unequal links and have the output on the opposite joint also mounted between two unequal links. This results in sideways motion. However, this would also result in parasitic transverse motion which would mean that the final motion would not be linear being their combination. Therefore, this last configuration will not be retained further.

Lets R be the longest link length, the links next to B, and r be the smallest link one, the links next to O_2.

Since this configuration is symmetric around the axis going through O_2 and B, it is thus possible to solve the problem geometrically by cutting the quadrilateral shape into two mirror triangles where the Pythagorean theorem will be applied to determine the distance between O_2 and B giving:

$$x = r\sqrt{1-\left(\sin\left(\frac{\theta}{2}\right)\right)^2} + R\sqrt{1-\frac{r\left(\sin\left(\frac{\theta}{2}\right)\right)^2}{R}} \tag{26}$$

This equation expresses then the forward kinematics problem.
Using the law of cosinuses on the general triangle where the longest side is that line between O_2 and B, it is possible to write a more compact version for the FKP:

$$x = \sqrt{R^2 - r^2 - 2r\cos\left(\tfrac{1}{2}\theta\right)} \tag{27}$$

The inverse kinematics problem requires the distance or position x as input which completes the two triangle lengths into the diamond shape. Hence, the cosinus laws on general triangles can be applied to solve the IKP:

$$\theta = 2\arccos\left(\frac{1}{2}\frac{R^2 - r^2 - x^2}{r}\right) \tag{28}$$

To obtain the differential kinematics models, the kinematics models are differentiated.
FDP:

$$v = \frac{1}{2}\frac{r^2\sin\left(\tfrac{1}{2}\theta\right)\omega}{\sqrt{R^2 - r^2 - 2r\cos\left(\tfrac{1}{2}\theta\right)}} \tag{29}$$

Differentiation of the IKP leads to the following IDP expression:

$$\omega = v^* \frac{4\sqrt{R^2 - r^2 - 2r\cos(\frac{1}{2}\theta)}}{r\sqrt{4 - 4\cos(\frac{1}{2}\theta)^2}} \tag{30}$$

After testing several approach for obtaining the differential model leading to accelerations, it was observed that starting with the inverse problem leads to more compact expressions:
The IDDP is obtained by differentiating the IDP:

$$\alpha = a(A1 + A2) \text{ where } A1 = \frac{4}{r\sqrt{4 - \frac{(R^2 - r^2 - x^2)^2}{r^2}}},\ A2 = -\frac{8x^2(R^2 - r^2 - x^2)}{r^3\left(4 - \frac{(R^2 - r^2 - x^2)^2}{r^2}\right)^{3/2}} \tag{31}$$

Inverting the IDDP produces the FDDP but it cannot be shown in the most compact form.
The Kite configuration models are definitely more elaborate and complex than for the rhombus configuration without necessarily leading to any kinematics advantages.

3.2.4 The rhombus configuration repetition or networking

The rhombus four-bar linkage can be multiplied as it can be seen in platform lifting devices. The repetition of these identical linkages helps reduce the encumbrance and this will be studied in this section in the context of linear actuator design.

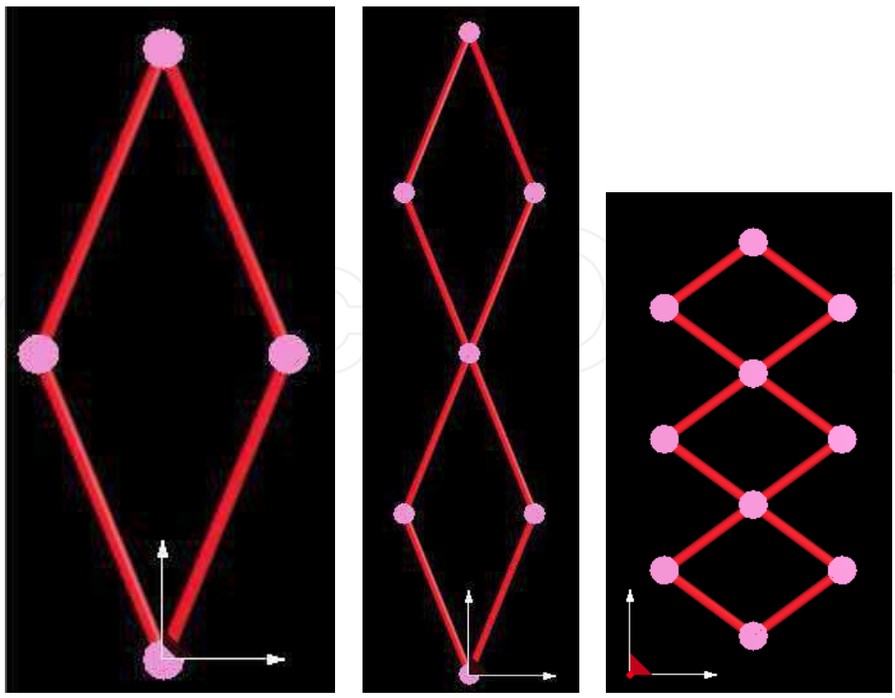

(a) Single rhombus (b) Double rhombus (c) Triple rhombus

Fig. 11. Rhombus networking

The distance traveled by the first moving central joint (FKP) is:

$$x_1 = 2r\cos\left(\frac{\theta}{2}\right) \tag{32}$$

This problem can be solved just like solving the original single rhombus FKP.
The distance traveled by the second moving central joint (FKP) is:

$$x_2 = 2x_1 = 4r\cos\left(\frac{\theta}{2}\right) \tag{33}$$

The impact of adding the second rhombus is doubling the distance or position reach.
The distance traveled by the third moving central joint or the solution of the FKP of a triple rhombus is:

$$x_3 = 3x_1 = 6r\cos\left(\frac{\theta}{2}\right) \tag{34}$$

This trend can be generalized to a repetition of n identical rhombuses.

$$x_n = nx_1 = n2r\cos\left(\frac{\theta}{2}\right) \tag{35}$$

The result of the four-bar rhombus repetition is the linear motion amplification by that repetition number.
To obtain the inverse kinematics problem, one can proceed with inversion of the FKP.
The double rhombus angular position of the actuator can then be deduced:

$$\theta = 2\arccos\left(\frac{1}{4}\frac{x}{r}\right) \tag{36}$$

This equation can then also be extrapolated to a repetition of n identical rhombuses.

$$\theta = 2\arccos\left(\frac{1}{2n}\frac{x}{r}\right) \tag{37}$$

The forward differential model is obtained by derivation of the forward kinematics model. For a double rhombus configuration, the relative speed of the second central joint is equal to the absolute speed of the first central joint:

$$v_{2/r} = v_1 \tag{38}$$

$$v_2 = v_1 + v_{2/r} \tag{39}$$

$$v_2 = 2v_1 \tag{40}$$

where

$$v_1 = -r\omega\sin\left(\frac{\theta}{2}\right) \tag{41}$$

Hence, the actual speed of the second extremity or the final end-effector becomes:

$$v_2 = -2r\omega\sin\left(\frac{\theta}{2}\right) \tag{42}$$

The impact of adding the second rhombus is doubling the end-effector velocity.
The same result would be obtained by derivation of the equation for x_2.
We now calculate the velocity of the third moving central joint which corresponds to the solution of the FDP of a triple rhombus.

$$v_3 = 3v_1 = -3r\omega\sin\left(\frac{\theta}{2}\right) \tag{43}$$

This trend can be generalized to a repetition of n identical rhombuses:

$$v_n = nv_1 = -nr\omega\sin\left(\frac{\theta}{2}\right) \tag{44}$$

The inverse differential model can be obtained in two ways, either by derivation of the inverse kinematics model or inversion of the forward differential model.
By inversion of the FDP, the double rhombus angular position of the actuator can then be deduced:

$$\omega = vr^{-1}\frac{1}{\sqrt{4-\frac{x^2}{r^2}}} \tag{45}$$

For the triple rhombus, we extrapolate:

$$\omega = v\frac{2}{3r}\frac{1}{\sqrt{4-\frac{x^2}{r^2}}} \tag{46}$$

For a linkage with the repetition of n rhombuses, we obtain the following equation:

$$\omega = v\frac{2}{nr}\frac{1}{\sqrt{4-\frac{x^2}{r^2}}} \tag{47}$$

To determine the accelerations, we will again differentiate the former differential models. We calculate derivation of the equation for v_2 for the second rhombus; it results in doubling the end-effector acceleration.
The FDDP for the case where we are doubling the rhombus leads to:

$$a_2 = 2a_1 = -2r\alpha\sin\left(\frac{\theta}{2}\right) - \frac{1}{2}r\omega^2\cos\left(\frac{\theta}{2}\right) \tag{48}$$

For the triple rhombus, we can determine that:

$$a_3 = 3a_1 = -3r\alpha\sin\left(\frac{\theta}{2}\right) - \frac{1}{2}r\omega^2\cos\left(\frac{\theta}{2}\right) \tag{49}$$

For n rhombuses, it is possible to extrapolate:

$$a_n = na_1 = -nr\alpha\sin\left(\frac{\theta}{2}\right) - \frac{1}{2}r\omega^2\cos\left(\frac{\theta}{2}\right) \tag{50}$$

Multying n times the rhombus linkage results in multiplying the acceleration likewise.
The IDDP, inverse model for a double rhombus, through derivation of the IDP or inversion of the FDDP, the calculation returns this equation:

$$\alpha = 2ar^{-1}\frac{1}{\sqrt{16-\frac{x^2}{r^2}}} - \frac{1}{8}v^2xr^{-4}\left(1-\frac{1}{16}\frac{x^2}{r^2}\right)^{-\frac{3}{2}} \tag{51}$$

For three rhombuses, the angular acceleration can then be determined:

$$\alpha = 2ar^{-1}\frac{1}{\sqrt{36-\frac{x^2}{r^2}}} - \frac{1}{2}7v^2xr^{-4}\left(1-\frac{1}{36}\frac{x^2}{r^2}\right)^{-\frac{3}{2}} \tag{52}$$

We have then extrapolated for a linear actuator constructed with n rhombuses:

$$\alpha = 2\frac{a}{nr}\frac{1}{\sqrt{4-\frac{x^2}{n^2r^2}}} - v^2xn^{-3}r^{-4}\left(1-\frac{1}{4}\frac{x^2}{n^2r^2}\right)^{-\frac{3}{2}} \tag{53}$$

3.2.5 The kite configuration repetition or networking

There seems to be no advantage to gain from networking the kite configuration. This will even add complexity to the kinematics models. Therefore, this prospect has not been investigated further.

4. Kinematics performance

4.1 Singularity analysis

4.1.1 General four bar linkage

For the general four bar linkage, singularities can be found when $A + C = 0$ using the values of equation 8. The solution to this equation results in:

$$\theta_2 = \arccos\left(\frac{1}{2}\frac{-2r_1 r_4 + {r_1}^2 + {r_2}^2 - {r_3}^2 + {r_4}^2}{r_2\left(-r_4 + r_1\right)}\right) \tag{54}$$

4.1.2 The parallelogram configuration

Singularities could be found only when $Rr = 0$ which is impossible since all links obviously have lengths larger then zero.

From the kinematics point of view, no limitations apply on the application of parallelograms since the rocker can follow the crank in any position allowing full rotation capability, therefore having no kinematics singularity whatesoever.

This mechanism could be considered somewhat similar or equivalent to the belt and pulley one where the two pulleys are of equal lengths if the belt is considered without elasticity.

4.1.3 The rhombus configuration

For the IDP, singularities exist and they can be determined by cancelling the denominator in the equations 20 and 21 leading to the two following equations.

The first one calculates the singularity in terms of the input angle θ:

$$\sin\left(\frac{\theta}{2}\right) = 0 \tag{55}$$

Hence, we find a singularity at $\theta = 0$ and its conterpart $\theta = 360$ degrees.

For the second one determines the singularity in terms of the extremity position x:

$$\sqrt{4 - \frac{x^2}{r^2}} = 0 \tag{56}$$

Hence, the singular position $x = 2r$ corresponds to the same posture as $\theta = 0$.

From a geometric point of view, links have no material existence (no mass) and they can occupy the same position in space. In reality, the masses do not allow such cases and therefore the singularity will be alleviated by bar width as will be explained later in the design section. The IDDP models bring singularities. Observation of the denominator allows us to determine that the singular configurations are just the same as the one studied for the IDP since the equations feature the same denominators under the power.

4.1.4 The kite or diamond shape configuration

If $R > r$, then this results then into an amplified motion without any singularity with full 360 degrees rotation of the input crank. This configuration has an advantage over the other

types of four-bars. This would surely represent one reason to apply this mechanism as a linear actuator.
If $R < r$, then the mechanism cannot reach an input angle of 180 degrees since this would mean $2R > 2r$ in contradiction with stated configurations. Hence, the system will block into position $\theta_{max} < 180°$ unable to go further. The angular range will be limited to $[0, \theta_{max}]$ where:

$$\theta_{max} = 2\arcsin\left(\frac{R}{r}\right) \tag{57}$$

This posture also yield a singularity which can also enforce mechanism blockage. Hence, this type will not be retained.

4.1.5 The rhombus configuration repetition or networking

In terms of singularities, finding the roots of the FDP and IDP will lead to the same singularities as for a single rhombus as it would seem logical. In terms of singularities, finding the roots of the FDDP and IDDP is equivalent to finding the same singularities solving the roots of only the IDDP as for a single rhombus.
Therefore, networking rhombuses will not introduce any singularity.

4.2 Workspace

The second important performance criterion for robotic design is usually the workspace. In the case of single DOF device, this narrows down to a simple range which we wish to maximize.

4.2.1 The general four-bar linkage

The mechanism can reach the following maximum length where two links are aligned, either r_1 and r_4 or r_2 and r_3. Then, the mechanism reach will be x_{max} and is calculated by the length of the extension of the two shortest links going from O_2 and leading to the extremity B:

$$x_{max} = \min\left(r_1 + r_4, r_2 + r_3\right) \tag{58}$$

The mechanism can also reach a minimum length which is a far more difficult problem to determine depending upon the configuration and relative link lengths. This is where Graschoff's formulas could help solve this problem. Despite the fact that link lengths value could be found leading to a coupler curve being a straight line, this constitutes another reason to avoid the general four-bar mechanisms.

4.2.2 The parallelogram configuration

The maximum and minimum actuator values of x can be determined by looking for the roots of the $x(\theta)$ function derivative or by geometric reasoning. Hence, using the simplest, i-e the second approach, we can determine that the extremas are found at $\theta = k\pi$ where $k \in \{0,1,2,3, \ldots\}$. With $n = 0$, the maximum value is found $x_{max} = R + r$ and with $n = 1$, the minimum value is $x_{min} = |R - r|$. We do not need to go further because of the repetitive nature of the trigonometric signal. These correspond to the posture where the four-bar is folded on itself: one fold to the left and one to the right.

4.2.3 The rhombus configuration

To determine the maximum and minimum values, several methods lead to the same results.

Taking the FKP, equation 14, the maximum value is obtained when $cos(\frac{\theta}{2}) = 1$ and the minimum value will be when $cos(\frac{\theta}{2}) = -1$. Hence, $x_{max} = 2r$ and the related angle is then $\theta = 0$. Moroever, $x_{min} = -2r$ and the related angle is then $\theta = -2\pi$. These values imply that the pure geometric nature of the kinematics analysis allows the mechanism to reverse by going unto itself. Hence, the minimum can be seen on the left or negative side of the reference frame and the maximum is located on the right or positive side.

With considerations of the linkage dimensions, the geometric analysis can be augmented by taking into account the linkage width.

Firstly, two linkages cannot occupy the same space, therefore, the rhombus linkage configuration will have a pair of opposite linkages below and one pair above. This lead to physical constraints equations. This property can also be translated into geometric information.

These opposite links are parallel pairs which will eventually touch each other alongside at two mechanism rotations. These postures could be considered as folded ones. The first corresponds to the minimum rotation and the second to the maximum rotation.

Let the rhombus linkage be constructed by four bars of identical width w.

The minimal rotation angle increases to:

$$\theta_{min} > 0 \tag{59}$$

$$\theta_{min} = 2\arcsin\left(\frac{w}{r}\right) \tag{60}$$

Taking into account that the kinematics chain cannot reverse by going unto itself, the maximal rotation angle reduces to:

$$\theta_{max} < \pi \tag{61}$$

$$\theta_{max} = 2\arccos\left(\frac{w}{r}\right) \tag{62}$$

The final range of the linear actuator is then the interval determined by: [2 $\arcsin(\frac{w}{r}$, 2 $\arccos(\frac{w}{r}$].

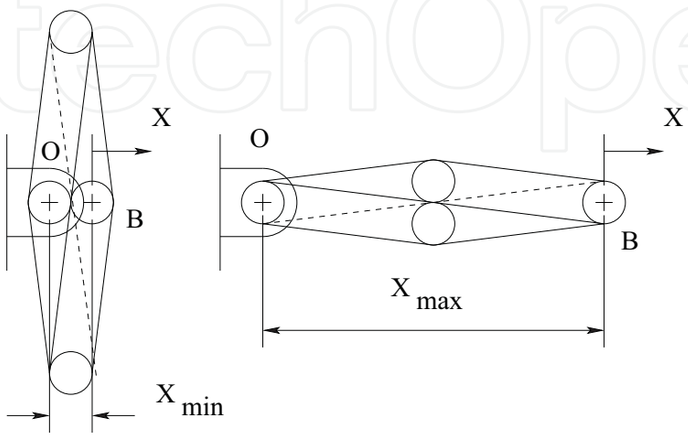

Fig. 12. The rhombus extreme positions

The extreme positions can be determined from these values. Minimal length is going to occur at maximal angular displacement.

$$x_{min} = 2r\cos\left(\frac{\theta}{2}_{max}\right) \tag{63}$$

Substituting θ_{max} into the equation, we get:

$$x_{min} = 2r\cos\left(2\arccos\left(\frac{w}{r}\right)\right) \tag{64}$$

Similarily, maximal length is going to occur at minimal angular displacement.

$$x_{max} = 2r\cos\left(\frac{\theta}{2}_{min}\right) \tag{65}$$

Substituting θ_{min} into the equation, we get:

$$x_{max} = 2r\cos\left(2\arcsin\left(\frac{w}{r}\right)\right) \tag{66}$$

4.2.4 The kite or diamond configuration

Let the kite linkage be constructed by four bars of identical width w.
The minimal rotation angle is exactly the same as the rhombus:

$$\theta_{min} > 0 \tag{67}$$

$$\theta_{min} = 2\arcsin\left(\frac{w}{r}\right) \tag{68}$$

Taking into account that the kinematics chain cannot reverse by going unto itself, the maximal rotation angle reduces to the case where the long bars touch each other in the negative sense of the reference frame. We have to take then the angle outside the triangle formed by these long bars:

$$\theta_{max} < 2\pi \tag{69}$$

$$\theta_{max} = 2\pi - 2\arcsin\left(\frac{w}{R}\right) \tag{70}$$

The extreme positions can be determined from these values. In the case of maximal position, the two geometric triangles formed by the long and short links add up:
Minimal length is going to occur at maximal angular displacement.

$$x_{min} = \sqrt{R^2 - (\frac{w}{2})^2} - r\cos\left(\frac{\theta}{2}_{max}\right) \tag{71}$$

Maximal length is going to occur at minimal angular displacement.

$$x_{max} = \sqrt{R^2 - (\frac{w}{2})^2} + r\cos\left(\frac{\theta}{2}_{max}\right) \tag{72}$$

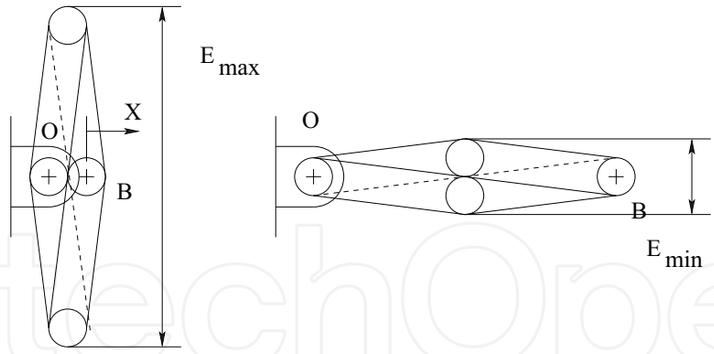

Fig. 13. The rhombus encumbrance

4.3 Encumbrance

4.3.1 The rhombus configuration

The proposed linear actuators are based on four-bar linkage where encumbrance becomes an issue considering that the mechanism spread sideways making them subject to collisions if other actuators would be located in the vicinity such as it is often the case with parallel manipulators.

Ecumbrance is defined as the distance from one side of the mechanism to the other side taking into account the linkage width.

A Rhombus would have minimum encumbrance of $E_{min} = 2w$ when the angle is at θ_{min}. This characteristic is relatively unimportant compared to the maximum encumbrance occuring at the maximum input angle posture θ_{max}:

$$E_{max} = 2\sqrt{r^2 - w^2} + w \tag{73}$$

4.3.2 The kite configuration

A folded kite would have minimum encumbrance of $E_{min} = 2w$ when the angle is at θ_{min} just like the rhombus. The maximum encumbrance is occuring at the maximum input angle posture $\theta_{max} = \frac{\pi}{2}$ when the smaller links are aligned:

$$E_{max} = 2r + w \tag{74}$$

As can be observed, the kite encumbrance only really depends on the dimension of the shortest links.

4.4 The repeated rhombus configuration

The problem of encumbrance justifies the design of a mechanism based on the repetition of identical rhombuses as it is done for lifting platforms.

The repetition of the four-bar rhombuses is not affecting the rotation input and the θ_{min} and θ_{max} values are only related to the first rhombus, therefore these extrema are unchanged.

4.4.1 The double rhombus

For the double rhombus, the minimum position is determined by:

$$x_{min} = 4r\cos\left(2\arccos\left(\frac{w}{r}\right)\right) \tag{75}$$

And the maximum position is calculated using:

$$x_{max} = 4r\cos\left(2\arcsin\left(\frac{w}{r}\right)\right) \tag{76}$$

4.4.2 The triple rhombus

For the triple rhombus, the minimum position is determined by:

$$x_{max} = 6r\cos\left(2\arcsin\left(\frac{w}{r}\right)\right) \tag{77}$$

And the maximum position is calculated using:

$$x_{max} = 6r\cos\left(2\arcsin\left(\frac{w}{r}\right)\right) \tag{78}$$

4.4.3 The multiple rhombus

For the generalized case with n rhombuses, the minimum position is determined by:

$$x_{max} = n2r\cos\left(2\arcsin\left(\frac{w}{r}\right)\right) \tag{79}$$

And the maximum position is calculated using:

$$x_{max} = n2r\cos\left(2\arcsin\left(\frac{w}{r}\right)\right) \tag{80}$$

4.4.4 Encumbrance of the multiple rhombus

The networking of rhombuses is not affecting encumbrance in the sense that the values are exactly the same. However, the main advantage is that the reach which can be defined as the maximum position is increasing while the encumbrance remains unchanged. This could not happen with a simple rhombus where we would need to increase the link lengths in order to increase reach resulting in larger emcumbrance.

Lets define the encumbrance ratio.

The encumbrance ratio is defined as the ratio of reach divided by the transverse encumbrance perpendicular to the axis of motion.

$$e = \frac{X_{max}}{E_{max}} \tag{81}$$

For the repeated rhombus, this occus when $\theta = \theta_{min}$ and the encumbrance ratio becomes:

$$e = n2r\cos\left(2\arcsin\left(\frac{w}{r}\right)\right)2\sqrt{r^2 - w^2} + w \tag{82}$$

Hence, the motion to encumbrance ratio is increasing proportionaly with the rhombus repetition.

5. Design examples

5.1 Initial prototypes

A first group of prototypes were constructed and tested using a Meccano set while the author was working at the Ecole Nationale des Arts et Metiers in Metz. This resulted in the constuction of a planar parallel manipulator as seen in figure 14. The DC motor was the typical Meccano 36 VDC.

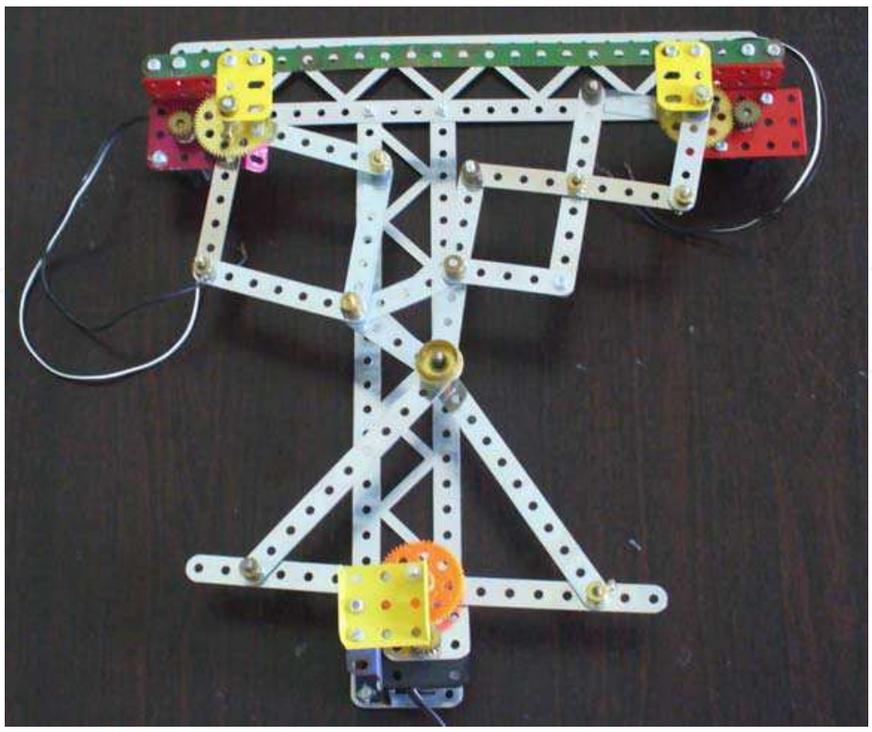

Fig. 14. Planar parallel manipulator with four-bar actuators

They were sufficient to prove and validate the concept. In effect, one rhombus four-bar with a Meccano motor could not be seen moving due to very high accelerations.

5.2 Actual prototypes

This work was then completed during the author stay at Middle East Technical University, Northern Cyprus Campus.

Three typical linear actuators were constructed as seen in figure 15. One comprising one rhombus, one with two rhombuses and one with a kite configuration using the same links and motors whenever possible.

5.2.1 Configuration

Here are the mechanism geometric parameters. They were constructed with two standardized bars. The short bars have length r = 10 cm and width w = 3 cm. The long bars have length R = 20 cm with same width.

The geared electrical motors were selected to provide maximum rotation speed of 120 RPM. Hence, $\omega_{max} = 4\pi$ radians/s.

5.2.2 Extreme positions

For the rhombus, from the proposed equations, the minimum input angle is then θ_{min} = 0,301 radian. The maximum input angle is θ_{max} = 2,84 radian. These values are confirmed by measurements on the prototypes.

From these angular positions, we calculate the maximum position or reach as x_{max} = 19,77 cm and the minimum value is x_{min} = 3 cm. Again these calculated values are confirmed by measurements.

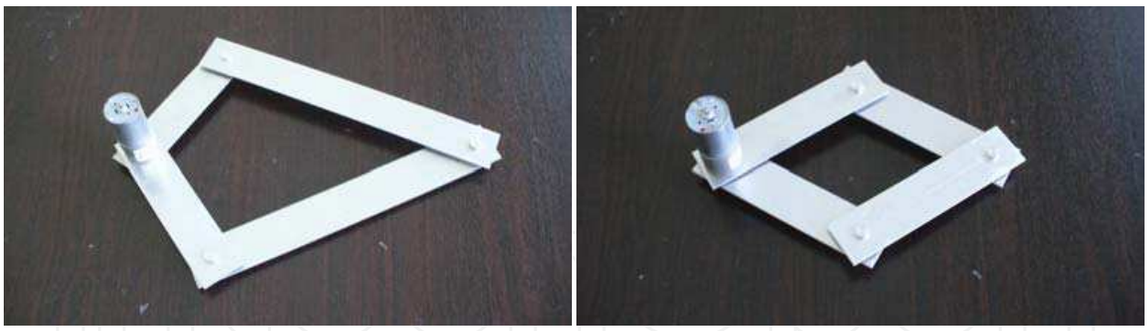

(a) Kite (b) Single rhombus

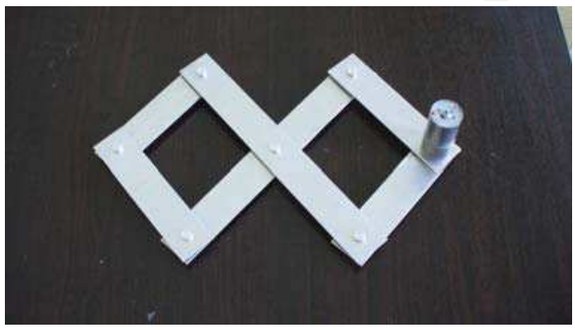

(c) Double rhombus

Fig. 15. The three four-bar actuator prototypes

The encumbrance can also be deduced. At θ_{max}, the maximum encumbrance is calculated as E_{max} = 22,77 cm. This was confirmed by measurements.

5.2.3 Motion analysis

In the curves of figure 16, t is in fact θ_2, the angular input position in radian, and ω is the angular velocity made to change from -4π to 4π radians/s.

The first question is about the actuator linearity and this issue can be answered by plotting the extremity position in relation to the input angle position. The motion becomes non-linear at the angular extremities and it becomes almost linear for a large number of angular positions from -1 to 1 radian corresponding to the position range of -18 to 18 cm.

The second question is to determine the extremity velocity profile according to input angle position at angular velocities going from the minimum until the maximum. This last value comes from the geared motor specifications. End-effector velocity changes almost linearly with the angular velocity but changes non-linearly with the angular position. It cancels out at angular extremities and it becomes maximal at $\theta = \pi$.

This velocity profile also corresponds to the accuracy profile. This means that for a predefined encoder accuracy located on the gearmotor shaft, the resulting extremity accuracy will be changing accordingly. One can foresee that the lowest accuracy is attained at $\theta = \pi$ and the best accuracies are achieved near the angular position extremities.

The third question involves the extremity acceleration in relation to input angle position at angular velocities going from the minimum until the maximum. We have to fix some angular acceleration and the value $1 rad/s^2$ has been selected arbitrarily. Extremity

acceleration changes non-linearily with the angular velocity. It changes almost linearily with the angular position. It reaches very high values when the linkage reaches very close to the maximum position.

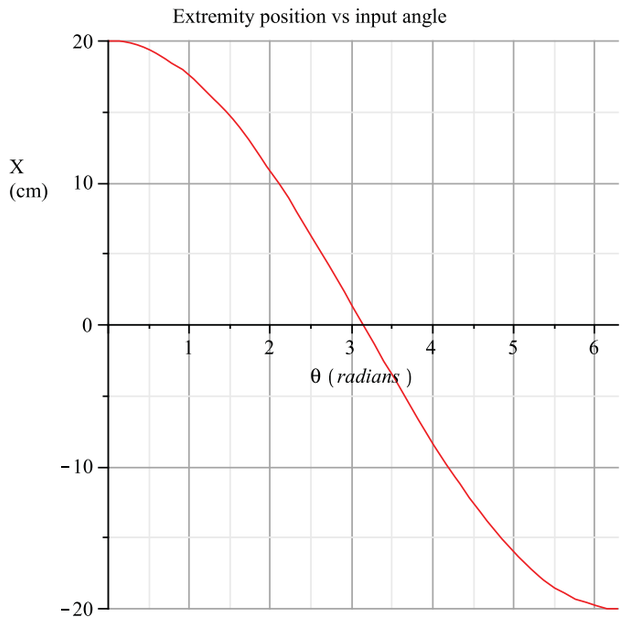

(a) Position

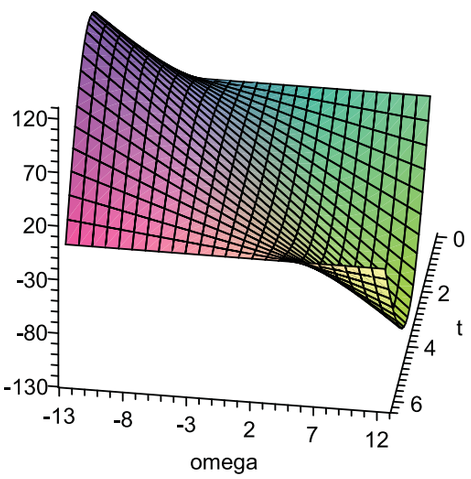

(b) Velocity

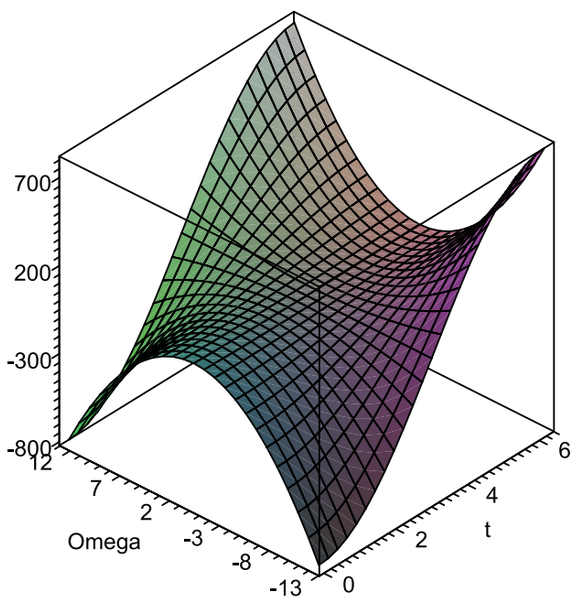

(c) Acceleration

Fig. 16. The rhombus kinematics performance

6. Conclusion

As can be seen by the results obtained by calculations as well by experiments on the prototypes, four-bar mechanisms can be rearranged in rhombus and kite configurations which lead to very performant prismatic pairs allowing to design very fast linear actuators. Moreover, to improve performance and to reduce emcumbrance, networking the rhombus four-bars can lead to very good results.
In the author's knowledge, this is the first time that four-bars were envisaged to be applied as linear actuators.
The next step will be to analyze their dynamics design integrating force analysis.
Then, to design a large scale parallel robot prototype will help investigate their worthiness towards the design a very high speed milling machine.
Finaly, several optimization problems may arise to determine proper linkage sizing.

7. References

Ceccarelli M. (1997) A new 3 d.o.f. spatial parallel mechanism. *Mechanism and Machine Theory*, vol.32(no.8), pp 896-902.

DaVinci, L. (1493) *Tratado de Estatica y Mechanica en Italiano.* CodexMadrid 1, National Library Madrid.

Euclid (2002) *Euclid's Elements - All thirteen books in one volume.* Green Lion Press. Based on Heath's translation, Greek original from c. 300 BC

Fichter, E.F., Kerr, D.R. and Rees-Jones, J. (2009) The Gough-Stewart platform parallel manipulator: a retrospective appreciation. *Proceedings of the Institution of Mechanical Engineers, Part C: Journal of Mechanical Engineering Science*, Volume 223, Number 1, pp. 243-281.

Gogu, G. (2004) Chebychev-Grübler-Kutzbach's criterion for mobility calculation of multiloop mechanisms revisited via theory of linear transformations. *European Journal of Mechanics - A/Solids*. Volume 24, Issue 3, May-June 2005, Pages 427-441

Gough, V. E. and Whitehall, S. G. (1962) Universal tyre testing machine. *Proceedings of the 9th International Automobile Technical Congress, discussion*, Federation Internationale des Societes dIngenieurs des Techniques de lAutomobile (FISITA) (Ed. G. Eley), (IMechE 1, London, UK), pp. 117137.

Kempe A.B. (1877) *How to draw a straight line; a lecture on linkages*. Macmillan and Co, London

Moon, F.C. (2007) *The Machines of Leonardo Da Vinci and Franz Reuleaux.* Volume on Kinematics of Machines from the Renaissance to the 20th Century, Series on History of Mechanism and Machine Science, Springer Netherlands, 417 pages

Reuleaux, F. (1876) *Kinematics of Machinery: Outlines of a Theory of Machines*. Macmillan and Co., London.

Rolland, L. (1998) Conception de mécanismes, élaboration des principes demobilit´e. Technical report number 98-02, ISR, EPFL, Lausanne.

Rolland, L. (1999) The Manta and the Kanuk novel 4-dof parallel mechanisms for industrial handling. *Proceedings of the ASME International Mechanical Engineering Congress*, Nashville, 14-19 Novembre 1999.

Scheiner, C. (1631) *Pantographice, seu ars delineandi res quaslibet per parallelogrammum lineare seu cavum, mechanicum, mobile*. Romae: Ex typographia Ludouici Grignani, sumptibus Hermanni Scheus, vol. 12, 108 pages.

Soylemez E. (1999) *Mechanisms.* METU Press, Ankara, 350 pages.

Uicker, J.J., Pennock, G.R. and Shigley, 2003, J.E. *Theory of Machines and Mechanisms, third edition*. Oxford University Press, New-York, 2003, 734 pages.

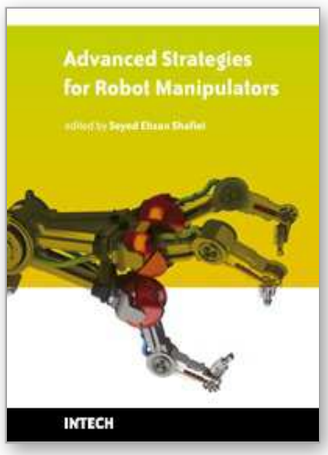

Advanced Strategies for Robot Manipulators

Edited by S. Ehsan Shafiei

ISBN 978-953-307-099-5
Hard cover, 428 pages
Publisher Sciyo
Published online 12, August, 2010
Published in print edition August, 2010

Amongst the robotic systems, robot manipulators have proven themselves to be of increasing importance and are widely adopted to substitute for human in repetitive and/or hazardous tasks. Modern manipulators are designed complicatedly and need to do more precise, crucial and critical tasks. So, the simple traditional control methods cannot be efficient, and advanced control strategies with considering special constraints are needed to establish. In spite of the fact that groundbreaking researches have been carried out in this realm until now, there are still many novel aspects which have to be explored.

How to reference

In order to correctly reference this scholarly work, feel free to copy and paste the following:

Luc Rolland (2010). Kinematics Synthesis of a New Generation of Rapid Linear Actuators for High Velocity Robotics, Advanced Strategies for Robot Manipulators, S. Ehsan Shafiei (Ed.), ISBN: 978-953-307-099-5, InTech, Available from: http://www.intechopen.com/books/advanced-strategies-for-robot-manipulators/kinematics-synthesis-of-a-new-generation-of-rapid-linear-actuators-for-high-velocity-robotics

INTECH
open science | open minds

InTech Europe
University Campus STeP Ri
Slavka Krautzeka 83/A
51000 Rijeka, Croatia
Phone: +385 (51) 770 447
Fax: +385 (51) 686 166
www.intechopen.com

InTech China
Unit 405, Office Block, Hotel Equatorial Shanghai
No.65, Yan An Road (West), Shanghai, 200040, China
中国上海市延安西路65号上海国际贵都大饭店办公楼405单元
Phone: +86-21-62489820
Fax: +86-21-62489821

IntechOpen